THE ASTROPHYSICAL JOURNAL, 464:516–520, 1996 June 10

SPECTROSCOPIC PROPERTIES OF THE H_3^+ MOLECULE: A NEW CALCULATED LINE LIST

LIESL NEALE AND STEVEN MILLER
Department of Physics and Astronomy, University College London, Gower Street, London, England WC1E 6BT, UK
AND
JONATHAN TENNYSON[1]
Institute for Theoretical Atomic and Molecular Physics, Harvard-Smithsonian Center for Astrophysics, 60 Garden Street, Cambridge, MA 02138
Received 1995 October 2; accepted 1995 December 6

ABSTRACT

A new list of H_3^+ infrared transition frequencies and intensities is presented. This list greatly extends the range of transitions considered to both higher energy and higher rotational states. The 3×10^6 transitions are found to significantly affect both the absorption coefficient of H_3^+ and its cooling properties at temperatures above 1000 K. It is hoped these new data will be used for models of cool stars of low metallicity, the giant planets, and other warm bodies composed largely of H_2.

Subject headings: infrared: general — line: identification — molecular data — planets and satellites: general — stars: atmospheres

1. INTRODUCTION

Much of the universe is made of hydrogen. At temperatures below a few thousand degrees kelvin this hydrogen is substantially molecular (Roberge & Dalgarno 1982). Molecular hydrogen, H_2, absorbs or emits only very weakly at infrared wavelengths. This means that cool bodies composed of hydrogen, such as metal-free stars or the giant planets, are strongly influenced by the properties of other, trace forms of hydrogen. For example, it is well known that the opacity of cool stars of low metallicity is dominated by the H^- ion (Ruiz, Bergeron, & Leggett 1993; Bergeron, Saumon, & Wesemael 1995; Allard & Hauschildt 1995).

The major ionic form of molecular hydrogen is H_3^+ which is formed rapidly by the reaction

$$H_2 + H_2^+ \rightarrow H_3^+ + H \,. \qquad (1)$$

H_3^+ has long been considered a vital component of the interstellar medium (Dalgarno 1994). More recently, H_3^+ emissions have been observed in Jupiter (Drossart et al. 1989), Uranus (Trafton et al. 1993), and Saturn (Geballe, Jagod, & Oka 1993) as well as probably in the remnant of SN 1987A (Miller et al. 1992). H_3^+ is also required in models of cool stars of low metallicity as a provider of electrons. However, so far it would appear that the global optical properties of H_3^+, either as an infrared opacity source or as a source of radiative cooling, have been largely ignored.

Kao et al. (1991) published an infrared line list of 699 H_3^+ transitions based on laboratory measurements augmented by ab initio calculations. This line list was designed as an aid to spectroscopic assignment rather than a comprehensive list for modeling purposes. For some time our group at UCL has maintained its own, more extensive (327,225 lines) line list from which the theoretical data of Kao et al. were drawn. For technical reasons, however, this line list was limited in its scope and, for example, did not include transitions involving high rotational excitation even in cases where such transitions had been observed in the laboratory.

Recently Neale & Tennyson (1995) have used a highly accurate, spectroscopically determined potential energy surface due to Dinelli, Polyansky, & Tennyson (1995a) to determine a new partition function for H_3^+. This partition function is 10–100 times larger than previous published estimates for temperatures above 4000 K. This increased partition function implies that substantial quantities of H_3^+ may be present in pure hydrogen atmospheres at these temperatures. If this is so, then the H_3^+ is liable to act, depending on circumstances, either as an absorber of infrared radiation or as a cooler via infrared emissions, as well as providing the electrons necessary to form H^- which heretofore has been considered the main opacity source in such objects.

To help quantify the importance of this behavior, we have computed a new and greatly extended (3×10^6 lines) H_3^+ line list. To do this we have developed new programs to overcome the technical limitations mentioned above. In this paper we present results showing that for $T > 1000$ K use of our new line list leads to greatly enhanced infrared absorption and/or emission by H_3^+ which we believe may prove important in a number of environments. It is neither possible or useful to present three million transitions in a journal such as this, so instead our line list is freely available in electronic form via ftp or the World Wide Web. Access and other details are given below.

The new list provides a database for individual transitions which supersedes that of Kao et al. (1991), which in any case is out of date because of the near doubling of available laboratory by data Majewski et al. (1994). Although the new line list is purely theoretical, it is of near spectroscopic accuracy. The differences between the calculated and laboratory transition frequencies should only be noticeable at resolutions greater than 20,000.

2. CALCULATIONS

The aim of our calculation was to consider all H_3^+ transitions lying at wavelengths longer than 1 μm. To this end it was considered necessary to treat all states lying at energies up to 15,000 cm^{-1} above the ground state at this system.

[1] Permanent address: Department of Physics and Astronomy, University College London, Gower Street, London, England WC1E 6BT, UK.

This energy is significantly higher than previous spectroscopic treatments and leads to new technical problems.

At low levels of excitation the H_3^+ ion vibrates about an equilateral triangle structure. However, above about 10,000 cm^{-1} it is possible for the molecule to sample linear geometries in which all three nuclei lie in a line. Under these circumstances the methods used for previous spectroscopic treatments of the system (Miller & Tennyson 1988; Kao et al. 1991) are no longer appropriate. This is because these finite basis representation (FBR) calculations employed basis functions which do not behave correctly for linear geometries. There are two aspects to this problem: finding a method to treat the linear geometries correctly and making a procedure computationally tractable for the large number of states that need to be considered.

All calculations were performed in scattering coordinates where r_1 represents an H–H distance and r_2 the distance of the third H to the "diatom" center of mass. The angle between r_1 and r_2 is θ. To maximize efficiency when H_3^+ goes above its barrier to linearity, the body-fixed z-axis was taken to be parallel to the r_1 coordinate (Tennyson 1993). Linear geometries are reached at $\theta = 0, \pi$, or $r_2 = 0$. It is the latter case which is the cause of problems at linearity as the Morse oscillator-like functions used for the r_2 coordinate in previous spectroscopic calculations (Miller & Tennyson 1988; Dinelli et al. 1995a) do not behave correctly for $r_2 = 0$ (Tennyson & Sutcliffe 1983).

A solution to this is to use spherical oscillator functions to represent the r_2 coordinate (Tennyson & Sutcliffe 1983). However, test FBR calculations with these functions (B. M. Dinelli & J. Tennyson, unpublished) showed very poor convergence properties. Alternative solutions were therefore sought. The solution to the computational problems is to use a method that is well adapted to obtaining many solutions to the nuclear motion problem such as the discrete variable representation (DVR) (Bačić & Light 1989).

Initially we adapted a mixed DVR-FBR method proposed by Bramley et al. (1994). This method employs spherical oscillators for the r_2 coordinate. These functions are explicitly coupled to the angular functions which leads to the correct boundary conditions at linearity being rigorously enforced. However, our tests showed that this method displayed poor convergence properties. This meant that complete calculations of the desired accuracy were simply too expensive computationally for us to contemplate.

We made a second attempt using Morse oscillator-like functions in a full DVR and correcting the misbehavior of these functions at $r_2 = 0$ by dropping DVR points with $r_2 < 0$ from our calculations. This approach is similar to one adopted by Watson (1994) for calculations of the low-lying states of H_3^+. Tests showed that these calculations gave results which oscillated about the correct answers. As these oscillations became increasingly violent as the calculations were "improved," this approach was abandoned.

We therefore performed the calculations entirely within a DVR using uncoupled spherical oscillators in the r_2 coordinate. Previous experience (Henderson, Tennyson, & Sutcliffe 1993; Tennyson 1993; Bramley et al. 1994) has shown that this method can give reliable results for the high-lying states of H_3^+ even though it does not rigorously enforce the correct boundary conditions for linear geometry.

Calculations were performed using the DVR3D program suite of Tennyson, Henderson, & Fulton (1995) with some minor improvements made to help us cope with the computational demands of the present calculations. We employed the spectroscopically determined effective H_3^+ potential energy surface of Dinelli et al. (1995a), the very accurate ab initio dipole surfaces of Röhse et al. (1994), and nuclear masses for the hydrogens.

DVR grids with 36, 40, and 32 points in the r_1, r_2, and cos θ coordinates, respectively, were used. These grids were based on the use of Morse oscillator-like functions for the r_1 coordinate and spherical oscillator functions for the r_2 coordinate, with $\alpha = 0$ for all calculations. Associate Legendre polynomials were used for the angular coordinate and were transformed from a DVR to an FBR during the calculation; see Tennyson (1993) for further details.

As states of A_1 symmetry have zero statistical weight ($g_{A_1} = 0$), "even" symmetry calculations which give these states were not attempted. Unfortunately, for technical reasons to do with the rotation-vibration calculations (Tennyson & Sutcliffe 1984), the H_3^+ states with "para" or E ($g_E = 2$) symmetry and "ortho" or A_2 ($g_{A_2} = 4$) symmetry could not be separately identified in the "odd" symmetry calculations performed. As will be discussed further below, ortho/para labels were hand-assigned to the most important transitions in our final line list.

We computed energies and wave function for all states up to 15,000 cm^{-1} above the ground state and with rotational angular momentum, $J \leq 20$. In the first "vibrational" step of the calculation, the lowest 700 energy solutions were selected from a 3000 dimension secular problem, and the lowest $500 \times (J + 1)$ solutions were used to solve the full ro-vibrational problem (see Tennyson et al. 1995).

It is important but difficult to estimate the convergence error for these calculations. Three methods were used to do this; comparison with our own FBR calculations for the low-lying states, comparison with the results of Carter & Meyer (1994), and self-consistent checks performed by repeating calculations with different parameters. Unfortunately, computational constraints meant that we could not afford to perform a complete set of such consistency checks. However, our estimate is that in the region up to 5000 cm^{-1} studied extensively previously our results are converged to about 0.05 cm^{-1}; this error rises to $\sim$0.2 cm^{-1} at 10,000 cm^{-1} and $\sim$1 cm^{-1} at 15,000 cm^{-1}. It should be noted that the reliability the effective potential employed probably behaves in a similar fashion.

The wave functions computed by the above procedure were then used to generate a list of all possible dipole transitions between them, subject only to rigorous selections rules on angular momentum ($\Delta J = 0, \pm 1$) and parity. Comparisons with transition intensities for low-lying transitions (1) calculated previously and (2) calculated with the present surfaces but the FBR TRIATOM program suite (Tennyson et al. 1993) gave excellent agreement. A measure of the reliability of our calculation is given by the fact that use of the line list has allowed us to assign and reassign many H_3^+ transitions previously measured in the laboratory. This work will be reported elsewhere (Dinelli et al. 1996).

From our initial line list of 3,187,125 transitions we removed all those which had an Einstein A-coefficient of less than 10^{-7} s^{-1}. The majority of these transitions arose from our inability to separate ortho and para states, and should have had zero line strength.

Our final line list, which is sorted by frequency and filed into wavelength regions, contains 3,070,571 transitions. A sample, covering the 3.529–3.547 μm spectral region, is

TABLE 1

H_3^+ TRANSITIONS IN THE 3.529–3.547 μm SPECTRAL REGION WITH $E'' < 5000$ cm^{-1} AND $A_{if} > 0.1$ s^{-1}

J'	E'/cm^{-1}	J''	E''/cm^{-1}	ω/cm^{-1}	A_{if}/s^{-1}	g
3.....	6016.843	4	3196.099	2820.7445	0.1092E+01	2
6.....	7319.702	7	4498.692	2821.0101	0.1284E+01	4
9.....	6586.906	8	3764.954	2821.9515	0.9389E+02	8/3
5.....	6327.767	6	3505.326	2822.4411	0.8053E+00	4
8.....	7008.598	7	4185.840	2822.7579	0.5941E+02	2
6.....	6794.479	6	3971.648	2822.8307	0.5701E+00	2
8.....	7720.904	7	4897.993	2822.9107	0.2078E+02	2
3.....	2928.318	2	105.176	2823.1423	0.4757E+02	2
8.....	7633.557	8	4810.271	2823.2855	0.1060E+02	2
2.....	5751.739	3	2928.318	2823.4210	0.4777E+01	2
5.....	6795.725	6	3971.648	2824.0771	0.1065E+01	2
7.....	7652.546	7	4827.900	2824.6459	0.2500E+01	2
8.....	7180.941	7	4356.114	2824.8270	0.5673E+02	2
5.....	6504.151	5	3679.061	2825.0901	0.6385E+01	4
5.....	5907.113	4	3081.159	2825.9541	0.1192E+03	4
3.....	2999.355	2	173.233	2826.1225	0.9174E+02	2
7.....	7151.655	6	4325.154	2826.5006	0.1854E+02	2
8.....	7556.342	7	4729.563	2826.7798	0.1547E+00	4
7.....	6799.370	6	3971.648	2827.7221	0.1575E+02	2
1.....	5520.111	2	2691.451	2828.6603	0.6454E+00	2
5.....	6025.693	4	3196.099	2829.5938	0.2063E+01	2
4.....	3081.159	3	251.225	2829.9337	0.1062E+03	4
4.....	3261.997	3	430.645	2831.3515	0.1065E+02	2
4.....	3196.099	3	363.898	2832.2009	0.4484E+02	2
4.....	6278.473	5	3446.024	2832.4488	0.3836E+01	2

given in Table 1. This region was chosen in part because it was extensively used to monitor the collision of comet Shoemaker-Levy 9 with Jupiter using UKIRT (Dinelli et al. 1995b). Even in this region, our complete list contains 430 transitions. Only the 26 transitions with $E'' < 5000$ cm^{-1} $A_{if} > 0.1$ s^{-1} are given.

The entire line list is available via either our group World Wide Web page on http://jonny.phys.ucl.ac.uk/home.html or anonymous ftp from jonny.phys.ucl.ac.uk (128.40.6.12) by looking in directory pub/astrodata/h3+. The list has been split into 16 files based on wavelength. File mλ_i.gz contains the transitions in the range $\lambda_i \leq \lambda < \lambda_{i'}$ where λ is the wavelength in microns. Thus, for example, transitions in the 3–3.5 μm region are in m3.gz. The files have been compressed using the standard Unix gzip utility.

3. RESULTS

As in the illustrative table, our line list is tabulated using the following parameters: J', E', J'', E'', ω, A_{if}, g. J', E' are the rotational quantum number and energy level of upper state; J'', E'' are the corresponding parameters for the lower state. In both cases energies, in cm^{-1}, are given relative to the lowest allowed state of H_3^+, the $J = 1$, $K = 1$ level of the vibrational ground state. This level is also the zero of energy in the fitted partition function given by Neale & Tennyson (1995).

The quantity $\omega (= E' - E'')$ is the transition frequency in cm^{-1}. A_{if} is the Einstein A-coefficient in s^{-1}. These can be converted into transition probabilities using the expression

$$|R|^2 = \frac{(2J'' + 1)}{(2J' + 1)} \frac{A_{if}}{\omega^3} . \quad (2)$$

In terms of transition probabilities, $|R|^2$, integrated absorption intensity, in cm^{-2} atm^{-1}, for each transition of frequency ω, in cm^{-1}, can be obtained from the expression

$$I = C \frac{\omega g (2J' + 1)}{Q(T)} \left[\exp\left(\frac{-E''}{kT}\right) - \exp\left(\frac{-E'}{kT}\right) \right] |R|^2 , \quad (3)$$

where the constant of proportionality, C, has the value 3.5656×10^7.

The quantity g in the parameter list and in equation (3) above is the nuclear spin degeneracy factor. For H_3^+ g should be 2 or 4. However, our calculation does not automatically make these assignments. We hand-assigned a few key states of H_3^+ and then used an algorithm based on transitions to obtain assignments for nearly all the transitions with $E'' < 5000$ cm^{-1} and J', $J'' \leq 10$, and some above these values. For levels which could not be unambiguously assigned, the high-temperature value, $g = 8/3$ (Sidhu, Miller, & Tennyson 1993), was used.

In equation (3), Q is the partition function. For H_3^+ reliable partition functions have been obtained for $T < 500$ K by Sidhu et al. (1991) and for 500 K $< T <$ 8000 K by Neale & Tennyson (1995).

To demonstrate the importance of our new line list we have computed integrated absorption intensities as a function of temperature. Figure 1 gives four examples. In these figures comparisons are made between Kao et al. (1991), S. Miller & J. Tennyson (unpublished) and this work. The plots of Figure 1 are actually histograms where the summed absorption intensity has been binned in boxes of width 25 cm^{-1}. In practice the width of the boxes acts to suppress the natural structure in the spectrum (Schryber, Miller, & Tennyson 1995), which may have important consequences when using our data for modeling. However, the enhanced structure in figures with more realistic box widths almost completely obscured the large differences given by using the different line lists, especially at higher temperatures.

In bodies such as the giant planets, H_3^+ appears to act as an important cooling agent; see, for example, Trafton et al. (1993). In this case the per molecule emission rate as a function of temperature is an important parameter which can be used to estimate the cooling effects of H_3^+ in a given atmosphere. Figure 2 gives these cooling functions, again calculated for the three line lists discussed above.

At high temperatures ($T > 4000$ K), a significant fraction of the occupied levels of H_3^+ is not included in our line list. A direct measure of the importance of the states neglected, as a function of temperature, can be obtained by comparing the partition function obtained by Neale & Tennyson (1995), who allowed for all levels of H_3^+, with the one calculated using the levels included in our line list. This ratio rises to about 3 at 8000 K. If one assumes that the states neglected in calculating the per molecule emission rate contribute pro rata, then one can simply scale the per molecule emission rate by the ratio of the complete to the effective partition function. The lower solid curve in Figure 2 gives our unscaled values; the upper solid curve is the scaled value. Below 3000 K, the two curves are indistinguishable.

4. DISCUSSION AND CONCLUSIONS

The absorption profiles in Figure 1 show that the spectrum of H_3^+ is dominated by three bands that broaden and eventually overlap with increasing temperature. The appearance of three bands is somewhat misleading. The

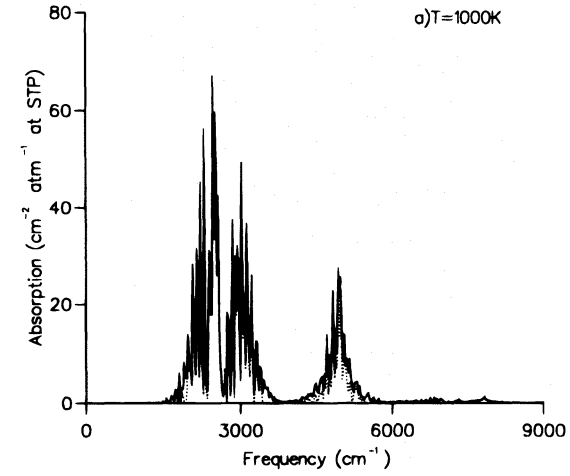

FIG. 1*a*

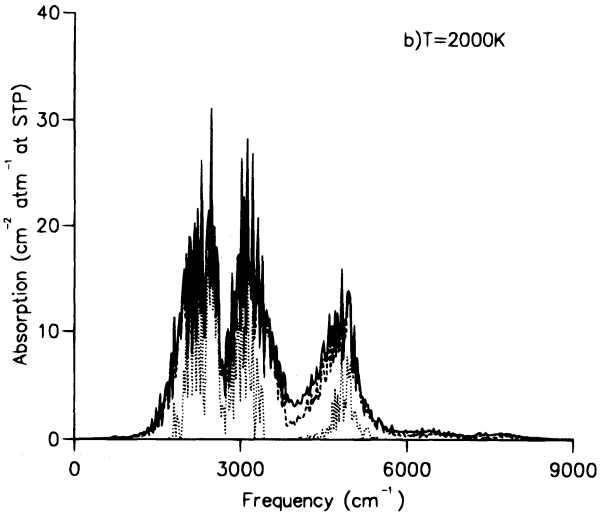

FIG. 1*b*

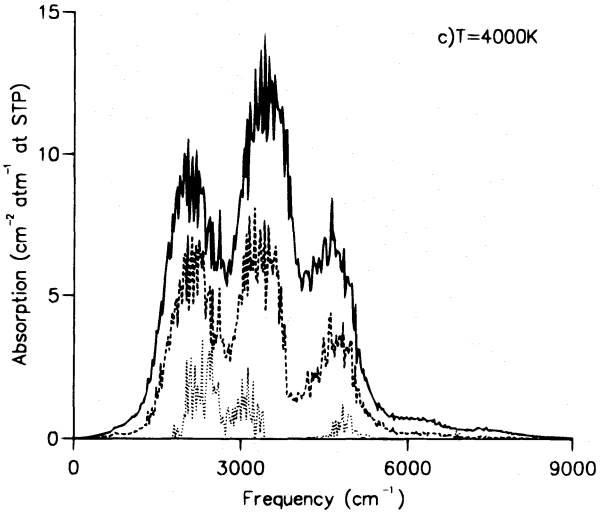

FIG. 1*c*

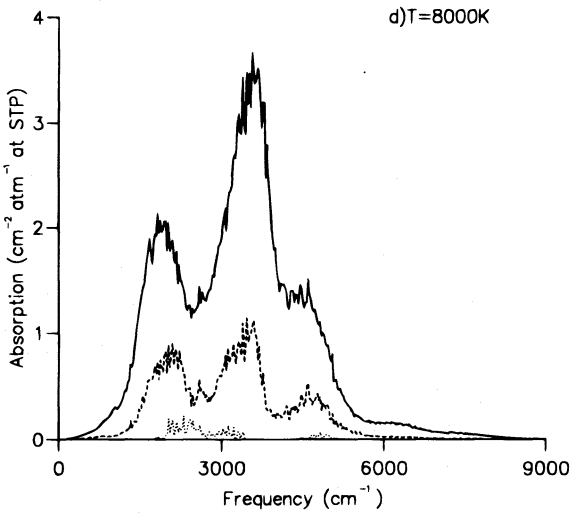

FIG. 1*d*

FIG. 1.—H_3^+ absorption cofficient as a function of temperature (*a*) 1000 K, (*b*) 2000 K, (*c*) 4000 K, and (*d*) 8000 K. The data have been binned in boxes of width 25 cm^{-1}. The dotted (*lowest*) curve was constructed using the line list given by Kao et al. (1991), the dashed (*middle*) curve used the data of Miller & Tennyson (unpublished), and the solid (*upper*) curve used the line list presented here.

band at 5000 cm^{-1} does indeed contain the rotational structure associated with a single vibrational transitions, the $2\nu_2$ overtone. The two other features are actually the *P*- and *R*-branch of the ν_2 fundamental. In fact, one can clearly identify the ν_2 *Q*-branch in Figure 1*a* as the strong feature just below the minimum.

Inspection of both Figures 1 and 2 shows that 1000 K (and below) the published data are sufficient for modeling H_3^+ absorption and emission; this is not true at higher temperatures. In particular, the absorption features shown when using our line list are significantly broader than those obtained using previous data. This can be attributed to the effect of the higher rotational states for which ab initio data were not previously available. The new line list suggests that H_3^+ absorbs over the entire range from 1800 cm^{-1} to 5500 cm^{-1} (5.5–1.8 μm). Similarly for temperatures above about 1000 K, H_3^+ is an efficient cooler.

Above about 4000 K it is clear that our raw calculations significantly underestimate the per molecule emissions of H_3^+ because of the (probably small individual) contributions from the high-lying states of H_3^+. In the case of per molecule emissions, we have been able to correct for these. This is harder when considering total absorption as a function of wavelength; however, it is not unreasonable to assume that a scaling similar to that used for the per molecule emissions would also work for the opacity.

The spectroscopy of H_3^+ is complicated. The molecule has many transitions, of varied intensity and irregular positions. It is important not to neglect the effect of the weaker transitions. For example, Kim et al. (1991) recorded auroral spectra of H_3^+ on Jupiter in the range 4.1–3.5 μm. They manually identified strong H_3^+ features and suggested that there was a structured background, later scaled down to $\sim$10% (Kim, Caldwell, & Herbst 1992), due to "methane haze." However, synthetic H_3^+ spectra using *all* H_3^+ lines in this spectral window can easily be made to account for the entire emissions eliminating the need to invoke methane at wavelengths shorter than 4 μm. Similar care must be taken

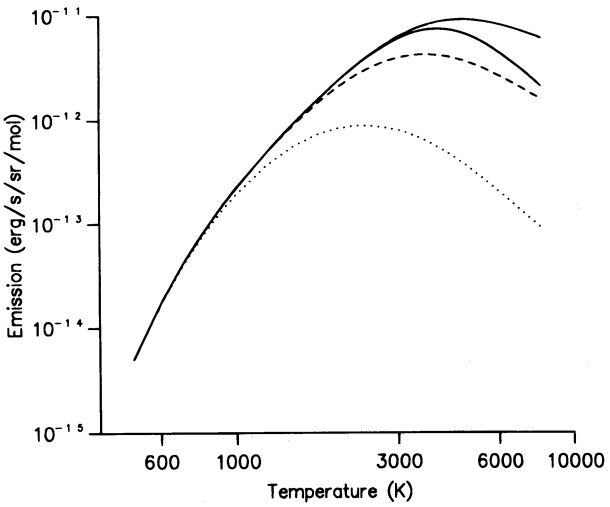

FIG. 2.—H_3^+ per molecule emissions as a function of temperature. The dotted (*lowest*) curve was constructed using the line list given by Kao et al. (1991), the dashed (*middle*) curve used the data of Miller & Tennyson (unpublished), and the solid (*upper*) curves used the line list presented here; see text for details.

when analyzing H_3^+ spectra from other sources such as Uranus.

In conclusion, we have computed a new H_3^+ line list containing approximately three million transitions. This line list is freely available in electronic form. To our knowledge the effects of H_3^+ opacity have never been included in stellar models. The substantial absorption predicted by our calculations in the infrared might have a significant effect on models of cool stars of low metallicity. We await the use of our data in such models with interest.

We thank Jeremy Schryber for his assistance with the absorption intensity calculations and Bianca Dinelli for many helpful discussions. This work has been supported by the UK Particle Physics and Astronomy Research Council and the National Science Foundation through a grant to the Institute for Theoretical Atomic and Molecular Physics at Harvard University and Smithsonian Astrophysical Observatory.

REFERENCES

Allard, F., & Hauschildt, P. H. 1995, ApJ, 445, 433
Bačić, Z., & Light, J. C. 1989, Ann. Rev. Phys. Chem., 40, 469
Bergeron, P., Saumon, D., & Wesemael, F. 1995, ApJ, 443, 764
Bramley, M. J., Tromp, J. W., Carrington, T., Jr., & Corey, G. C. 1994, J. Chem. Phys., 100, 6175
Carter, S., & Meyer, W. 1994, J. Chem. Phys., 100, 2104
Dalgarno, A. 1994, Adv. Atomic Molec. Opt. Phys., 32, 57
Dinelli, B. M., Polyansky, O. L., & Tennyson, J. 1995a, J. Chem. Phys., 103, 10,433
Dinelli, B. M., et al. 1995b, in Proc. European SL-9/Jupiter Workshop, ed. R. West and H. Böhnhardt (Garching: ESO), 245
Dinelli, B. M., Neale, L., Polyansky, O. L., & Tennyson, J. 1996, J. Molec. Spectrosc., to be submitted
Drossart, P., et al. 1989, Nature, 340, 539
Geballe, T. R., Jagod, M.-F., & Oka, T. 1993, ApJ, 408, L109
Henderson, J. R., Tennyson, J., & Sutcliffe, B. T. 1993, J. Chem. Phys., 98, 7191
Kao, L., Oka, T., Miller, S., & Tennyson, J. 1991, ApJS, 77, 317
Kim, S. J., et al. 1991, Nature, 353, 536
Kim, S. J., Caldwell, J., & Herbst, T. M. 1992, Icarus, 96, 143
Majewski, W. A., McKellar, A. R. W., Sadovski, D., & Watson, J. K. G. 1994, Canadian J. Phys., 72, 1016
Miller, S., & Tennyson, J. 1988, ApJ, 335, 486
Miller, S., Tennyson, J., Lepp, S., & Dalgarno, A. 1992, Nature, 355, 420
Neale, L., & Tennyson, J. 1995, ApJ, 454, L165
Röhse, R., Klopper, W., Kutzelnigg, W., & Jaquet, R. 1994, J. Chem. Phys., 101, 2231
Roberge, W., & Dalgarno, A. 1982, ApJ, 255, 176
Ruiz, M.-T., Bergeron, P., & Leggett, S. K. 1993, in White Dwarfs: Advances in Observation and Theory, ed. M. A. Barstow (Dordrecht: Kluwer), 245
Schryber, J. H., Miller, S., & Tennyson, J. 1995, J. Quant. Spectrosc. Rad. Transf., 53, 373
Sidhu, K. S., Miller, S., & Tennyson, J. 1992, A&A, 255, 453
Tennyson, J. 1993, J. Chem. Phys., 98, 9658
Tennyson, J., Henderson, J. R., & Fulton, N. G. 1995, Comput. Phys. Comm., 86, 175
Tennyson, J., Miller, S., & Le Sueur, C. R. 1993, Comput. Phys. Comm., 75, 339
Tennyson, J., & Sutcliffe, B. T. 1983, J. Molec. Spectrosc., 101, 71
———. 1984, Molec. Phys., 51, 887
Trafton, L. M., Geballe, T. R., Miller, S., Tennyson, J., & Ballester, G. E. 1993, ApJ, 405, 761
Watson, J. K. G. 1994, Canadian J. Phys., 72, 702